Fluid Phase Equilibria 427 (2016) 1–8

Contents lists available at ScienceDirect

Fluid Phase Equilibria

journal homepage: www.elsevier.com/locate/fluid

Binary mixtures of fatty acid ethyl esters: Solid-liquid equilibrium

Laslo A.D. Boros [a], Marta L.S. Batista [b], J.A.P. Coutinho [b], M.A. Krähenbühl [a], Antonio J.A. Meirelles [c], Mariana C. Costa [d, *]

[a] LPT, Department of Processes and Product Design (DDPP), School of Chemical Engineering (FEQ), University of Campinas (UNICAMP), 13083-852, Campinas, São Paulo, Brazil
[b] CICECO, Departamento de Química da Universidade de Aveiro, 3810-193, Aveiro, Portugal
[c] EXTRAE, Department of Food Engineering (DEA), School of Food Engineering (FEA), University of Campinas (UNICAMP), 13083-862, Campinas, São Paulo, Brazil
[d] LEF, Department of Processes and Products Design (DDPP), School of Chemical Engineering (FEQ), University of Campinas (UNICAMP), 13083-852, Campinas, São Paulo, Brazil

ARTICLE INFO

Article history:
Received 8 March 2016
Received in revised form
13 June 2016
Accepted 20 June 2016
Available online 23 June 2016

Keywords:
Cloud point
Solid-liquid equilibrium
Fatty acid ethyl ester (FAEE)
Biodiesel
Predictive UNIQUAC

ABSTRACT

Biodiesel is a renewable fuel that is commonly used in diesel engines around the world mostly in blends with the conventional diesel. There are many studies concerning its production and its properties and a series of them confirms the biodiesel advantages when compared with conventional diesel in relation of the environmental impacts. In spite of many advances concerning the biodiesel production and properties its behavior at low temperatures is worst than the conventional diesel, and, unfortunately, low temperature property information concerning fatty acid ethyl esters (FAEE) and the biodiesel is still scarce for researchers. This paper presents nine solid-liquid phase diagrams of FAEE binary mixtures to complement the studies of FAEE phase diagram previously reported. All of the phase diagrams have been determined using differential scanning calorimetry (DSC) and also modelled using both the Predictive UNIQUAC and the ideal solution models. The results have been shown good correlation between experimental and modelled data.

© 2016 Elsevier B.V. All rights reserved.

1. Introduction

Biodiesel is a biofuel obtained from animal or vegetable oils and fats by a transesterification reaction employing short chain alcohols, for instance, ethanol or methanol. It is more environmentally friendly than conventional diesel because is produced from renewable resources, is less toxic, generates less gas emissions and it is biodegradable [1,2]. Considering the biodiesel properties compared with conventional diesel the former presents higher flash points, good lubricity [3] and similar specific gravity, heat of combustion and kinematic viscosity [4]. These characteristics enable the use of biodiesel and biodiesel blends with conventional diesel in diesel engines without changes.

Physicochemical properties like as vapour pressure [5,6], Flash point [7], densities and viscosities [8–11] and equilibrium data of biodiesel and its components, namely fatty acids methyl esters (FAME) or FAEE [12–14] have been determined with the objective to improve the biodiesel production and its use as energy source.

Unfortunately, the biodiesel properties at low temperatures do not favour their use in diesel engines, difficult its storage and transportation, and create a poor low temperature behavior in its blends with conventional diesel [15,16]. Problems due to nucleation and growing of solid crystals appear around 275 K in biodiesel while in conventional diesel they appear at around 260 K [4]. Some tests are used to characterize the biodiesel behavior at low temperatures in which most important are the cold filter plugging point (CFPP), pour point (PP) and cloud point (CP). The former is given at a temperature in which fuel filters and lines become plugged [17] (EN 116, IP-309, ASTM D-6371), the second is the lowest temperature that is possible to the fuel to be pumped or just to flow [4] (ASTM D-97, ASTM D-5949) and the last one, the CP, is a temperature determined for the crystals to become visible and to form a hazy or cloudy suspension [4] (EN 23015, ASTM D-2500).

* Corresponding author. School of Chemical Engineering (FEQ), Albert Einstein Avenue 500, 13083-852, Campinas, São Paulo, Brazil.
E-mail addresses: laslo@petrobras.com.br (L.A.D. Boros), batista.m@ua.pt (M.L.S. Batista), jcoutinho@ua.pt (J.A.P. Coutinho), mak@feq.unicamp.br (M.A. Krähenbühl), tomze@fea.unicamp.br (A.J.A. Meirelles), mcosta@feq.unicamp.br (M.C. Costa).

http://dx.doi.org/10.1016/j.fluid.2016.06.039
0378-3812/© 2016 Elsevier B.V. All rights reserved.

These properties are closely monitored to ensure the operation without problem in cold climates [4]. Beyond the cold flow properties the knowledge of biodiesel and its compounds behavior under low temperatures are interesting to development of purification and/or separation processes and equipment design [18], as well as the knowledge are necessary to help to looking for compounds that can be employed to improve this properties [19,20].

This work complements and completes the study of the solid-liquid phase diagrams for binary mixtures of FAEE [21–26]. In this article nine new binary mixtures were measured employing a Differential Scanning Calorimetry (DSC) and are presented for the first time in the literature. A discussion on the type of phase diagram presented by these systems and its relation with the differences in chain length and melting temperatures of the two mixture components is carried. Since most binary mixtures of FAEEs are simple eutectics the *liquidus* line of the mixtures was here modelled employing the predictive UNIQUAC model and an ideal solution model.

2. Experimental section

The binary samples were prepared using high purity FAEE (min 99%) supplied from Nu-Chek Prep, INC. and handled as received. Each mixture component was weighed on an analytical balance (±0.2 mg), melted in a nitrogen atmosphere under stirring and stored in a refrigerator until its use in MDSC 2920 calorimeter of TA Instruments. The calorimeter was calibrated through small amount of high-purified indium (99.99%), cyclohexane (min 99.9%) and naphthalene (min 99%). Indium purity validated by TA Instruments and cyclohexane and naphthalene were supplied by Merck. The calibration and analyses occurs in the temperature range between 200 K and 600 K using the TA Instruments refrigerated cooling system and according to a methodology described in previous studies [21,27].

The accuracy of the experimental melting point data was estimated at the repeated run basis and executed with the calibration substances and some chosen mixtures [27]. The deviation on the measured temperature is no higher than 0.3 K.

3. Modeling

The predictive UNIQUAC model was chosen to describe experimental *liquidus* lines. This approach was previously applied to diesels and crude oils [28,29], to fatty acids [30], fatty acid methyl esters [18], fatty acid ethyl esters [21,27,31]and for biodiesel behavior at low temperatures [32,33].

Equation (1) is a simplified form of the equation generally used to describe the solid-liquid equilibrium [27].

$$\ln\frac{x_i^s\gamma_i^s}{x_i^l\gamma_i^l} = \frac{\Delta_{fus,i}H_i}{RT_{fis,i}}\left(\frac{T_{fus,i}}{T}-1\right) \tag{1}$$

The liquid and solid phase activity coefficients (γ_i^l, γ_i^s) were described by means of UNIFAC model [34] and a new predictive UNIQUAC model version written as [29,35].

$$\frac{g^E}{RT} = \sum_{i=1}^{n} x_i \ln\left(\frac{\Phi_i}{x_i}\right) + \frac{Z}{2}\sum_{i=1}^{n} q_i x_i \ln\left(\frac{\theta_i}{\Phi_i}\right) - \sum_{i=1}^{n} x_i q_i \ln\left[\sum_{j=1}^{n}\theta_j \exp\left(-\frac{\lambda_{ij}-\lambda_{ii}}{q_i RT}\right)\right] \tag{2}$$

with

$$\theta_i = x_i q_i \Big/ \sum_j x_j q_j \quad \text{and} \quad \Phi_i = x_i r_i \Big/ \sum_j x_j r_j \tag{3}$$

The predictive local composition concept [36] allows for estimation of the interaction energies (λ_{ij}) used by this model, without fitting to the experimental data. The pair interaction energies between two identical molecules are estimated from the enthalpy of sublimation of the pure crystalline component

$$\lambda_{ii} = -2/Z(\Delta_{sub}H_i - RT) \tag{4}$$

where Z is the coordination number ($Z = 10$). The enthalpies of sublimation ($\Delta_{sub}H = \Delta_{vap}H + \Delta_{fus}H$) are calculated at the melting temperature of the pure component.

The pair interaction energy between two non-identical molecules is given by

$$\lambda_{ij} = \lambda_{ji} = \lambda_{ii} \tag{5}$$

where i is the compound with the shorter alkyl chain of the pair ij.

As an alternative, a simpler approach for the description of the *liquidus* line measured in this study was also tested. It was assumed that the solid phase formed was essentially a pure fatty ester, and that the liquid phase was ideal. Based on these assumptions the relation between the composition of the mixture, x_i, and the melting/cloud point, T, was given by the classical solid-liquid equilibrium equation.

$$x_i^L = \exp\left[-\left(\frac{\Delta_{fus}H_i}{R}\left(\frac{1}{T}-\frac{1}{T_{fus,i}}\right)\right)\right] \tag{6}$$

The models used to calculate the solid-liquid equilibrium are totally predictive employing just the property of pure components to estimate the behavior of each phase. These properties were correlated in a previous paper [33] and are presented in Table 1. To the fusion ($\Delta_{fus}H$) and vaporization enthalpies ($\Delta_{vap}H$) of FAEE the correlations are presented in Equations (7) and (8) [33] and the melting temperatures (T_{fus}) were got from the thermograms.

$$\Delta_{fus}H = 3.92C_n + 16.80 \tag{7}$$

$$\Delta_{vap}H = 4.9C_n + 9.0 \tag{8}$$

In Equations (7) and (8) the enthalpy units are kJ mol^{-1}. It was considered that the differences between the fusion enthalpy ($\Delta_{vap}H$) and vaporization enthalpy ($\Delta_{fus}H$) of FAEE may be the same as those observed for the methyl esters [33].

4. Results and discussion

Nine phase diagrams of FAEE binary mixtures are presented to complement previous studies [21–26]. Table 1 presents the experimental melting temperature data as well as the calculated melting enthalpy of each FAEE content in the binary mixtures [33]. In previous studies the phase diagrams of ethyl stearate with ethyl linoleate, ethyl oleate, ethyl palmitate, ethyl myristate, ethyl laurate, ethyl caprate and ethyl caprylate [21] and ethyl palmitate with ethyl linoleate, ethyl oleate, ethyl palmitate, ethyl myristate, ethyl laurate, ethyl caprate and ethyl caprylate [22] were presented performing a total of 13 binary systems. Recently Robustillo et al. studied some FAEE ternary systems formed by ethyl palmitate, ethyl myristate and ethyl laurate [23], ethyl stearate, ethyl palmitate and ethyl laurate [24], ethyl oleate, ethyl palmitate and ethyl laurate [25], and ethyl oleate, ethyl myristate and ethyl stearate [26]. In their studies the authors also discuss in detail the solid

phase of the binary systems formed by the mentioned FAEE.

Table 2 show the melting temperatures of the pure FAEE studied and the data presented in literature. The Average Relative Deviation (ARD) was calculated between the our experimental data and literature data according to Equation (9), where N is the number of observations. ARD calculated for melting temperature was equal to 0.73%, confirming that there are a good agreement between our experimental melting temperature data and those found in literature.

$$ARD = \left(\frac{1}{n}\sum_{i=1}^{n}\left|\frac{T_{i,thiswork} - T_{i,literature}}{T_{i,thiswork}}\right|\right) \times 100 \quad (9)$$

The discussion of the new set of binary mixtures here presented divided in three subsections to allow a better discussion of the phase diagrams. A comparison with data previously reported [21–26] is carried for completeness.

4.1. Phase diagrams with ethyl caprylate

The *liquidus* lines of three saturated FAEE binary mixtures that content ethyl caprylate as one of the compounds are presented in Fig. 1 and reported in Table 3. The mixtures of ethyl palmitate + ethyl caprylate and ethyl stearate + ethyl caprylate were previously reported [21,22] as mentioned and are here represented for completeness.

The phase diagrams of ethyl caprylate with a saturated FAEE are very simple, as shown in Fig. 1, exhibiting a well defined eutectic point at $x_{caprylate} \cong 0.85$ for the ethyl caprate + ethyl caprylate binary mixture. The ethyl laurate + ethyl caprylate binary mixture seems, according to the model and experimental data, to exhibit a eutectic point at a composition of $x_{caprylate} \cong 0.96$. For the other systems represented in the same Figure it is impossible to define the temperature or concentration of the eutectic point that is located very close to the pure compound. Other way to verify the eutectic composition and/or the formation of a solid solution is through Tammann plot [37,38], a plot that associates the enthalpy of the eutectic reaction as a function of the sample composition. Tammann plots were sketched for each system of Fig. 1 and are presented in Fig. 2 (from a to e). It is interesting to note in all plots of Fig. 2 that eutectic enthalpies tends to zero in a concentration of ethyl caprylate of 0.05, approximately, for all binary systems suggesting that all of these five systems form a solid solution in the region of high concentration of heavier FAEE. The Tammann plot of ethyl laurate + ethyl caprylate binary mixture does not allow to conclude anything about the occurrence of the eutectic point of such a system due to the inexistence of an experimental point with a composition around 0.95 of ethyl caprylate. The same is true for the other 3 systems formed by ethyl myristate, ethyl palmitate and ethyl stearate with ethyl caprylate, but in the case of these systems the sample composition of the eutectic point should be very close to the pure ethyl caprylate in such a way that we will attain on experimental and technical limitation.

As discussed before [21,22] the addition of an FAEE with lower melting point in another FAEE that has higher melting point does not cause a relevant reduction of the mixture melting temperature. As can be observed in Fig. 1 a decrease of 10° on melting temperature of the mixture is observed only for concentrations of the lighter FAEE higher than 50%.

4.2. Phase diagrams with ethyl caprate

The phase diagrams formed by saturated FAEE with ethyl caprate are presented in Fig. 3 and melting and transitions temperatures are reported in Table 4. They show a very similar behavior with the previous set of data presented. In the systems formed by FAEE + ethyl caprate the eutectic point is clearly observed for systems ethyl laurate + ethyl caprate in a composition approximately equal of $x_{caprate} \cong 0.80$, ethyl myristate + ethyl caprate in a composition approximately equal $x_{caprate} \cong 0.90$ and the model results suggest the existence of a eutectic point in a composition approximately equal $x_{caprate} \cong 0.98$ for the system ethyl palmitate + ethyl caprate [22]. In the same way of the systems discussed in the previous section, FAEE + ethyl caprylate, the increase of two carbon atoms from system formed by ethyl caprate + ethyl laurate to four carbon atoms of the systems formed by ethyl caprate + ethyl myristate shift the eutectic point location in a molar fraction unit equal to 0.1. An increment of two more carbon atoms observed in the system by ethyl caprate + ethyl palmitate, does not allow the experimental observation of the eutectic point although the model results suggests its presence at a composition of $x_{caprate} \cong 0.98$ as mentioned [22].

Fig. 4 shows the Tammann plots of these four systems and suggest that in the phase diagram region that is rich in the heavier FAEE has a solid solution formation in the case of ethyl caprate + ethyl laurate and ethyl caprate + ethyl myristate mixtures but not for ethyl caprate + ethyl palmitate and ethyl caprate + ethyl stearate mixtures. These results denote that the solid solution formation is not only connected with the difference in the carbon chain but also with the molecular size of each component that makes up the mixture. All systems formed by FAEE + ethyl caprylate present a solid solution formation in a region rich in the heavier FAEE even when the difference between the carbon chain of the binaries FAEE mixtures is equal to 10 whereas

Table 1
Purities and thermophysical properties of FAEE used in this work.

Chemical name (usual name)	CAS number	Mass fraction purity[a]	r	q	T_c (K)	P_c (bar)	ω	$\Delta_{vap}H$ (kJ mol^{-1})[b]	$\Delta_{fus}H$ (kJ mol^{-1})[b]	$T_{melting}$ (K)[c,d]
Ethyl octanoate (ethyl caprylate)	106-32-1	>0.99	7.525	6.356	656.39	21.60	0.628	58.0	22.40	230.35
Ethyl decanoate (ethyl caprate)	110-38-3	>0.99	8.8738	7.436	690.216	18.46	0.709	67.8	30.23	254.51
Ethyl dodecanoate (ethyl laurate)	106-33-2	>0.99	10.2226	8.516	719.13	15.97	0.787	77.6	38.07	272.59
Ethyl tetradecanoate (ethyl myristate)	124-06-1	>0.99	11.5714	9.596	744.27	14.02	0.862	87.4	45.91	287.37
Ethyl hexadecanoate (ethyl palmitate)	628-97-7	>0.99	12.9202	10.676	766.41	12.43	0.935	97.2	53.75	297.01
Ethyl octadecanoate (Ethyl stearate)	124-06-1	>0.99	14.269	11.756	786.12	11.12	1.005	107.0	61.60	307.93
Ethyl (Z)-octadec-9-enoate (ethyl oleate)	111-62-6	>0.99	14.0369	11.543	771.07	11.12	1.013	107.3	25.39	254.61
Ethyl (Z,Z)-octadec-9,12-dienoate (ethyl linoleate)	544-35-4	>0.99	13.8048	11.33	785.89	11.57	1.008	108.9	24.39	220.68

[a] As reported by the supplier (Nu-Chek Prep, INC).
[b] Calculated melting enthalpies according previous work presented by Lopes et al. (2009) [33].
[c] Peak top temperature from DSC thermograms.
[d] Uncertainties for experimental melting temperatures are ±0.30 K.

Table 2
Comparison between melting temperatures presented in this study and those found in literature.

FAEE	$T_{melting}$ this work[a] (K)	$T_{melting}$ Literature (K)	FAEE	$T_{melting}$ this work[a] (K)	$T_{melting}$ Literature (K)
Ethyl caprylate	230.35	228.41 [41]	ethyl caprate	254.51	252.71 [41]
		230.35 [22]			254.51 [22]
		229.17 [21]			254.1 [21]
		230.05[b]			253.15[b]
		228 [42]			253.25[b]
ethyl laurate	272.59	271.37 [41]	ethyl myristate	287.37	285.67 [41]
		272.59 [22]			287.37 [22]
		272.31 [21]			286.98 [21]
		273.2 [23]			287.23 [23]
		263.15[b]			285.45[b]
		257.65[b]			284.15[b]
		262.5 [42]			285.9 [42]
Ethyl palmitate	297.01	296.38 [41]	ethyl stearate	307.93	306.13 [41]
		297.69 [22]			307.63 [21]
		297.92 [21]			307.4 [24]
		298.23 [23]			306.55[b]
		297.15[b]			306.65[b]
		292.45[b]			307.2 [42]
		296.35[b]			306.9 [42]
		297.7 [42]			304.05 [42]
		297.15 [42]			306.55 [42]
		298.2 [42]			304.3 [42]
		295.2 [42]	ethyl oleate	254.61	252.83 [41]
		295.2 [42]			255.12 [22]
Ethyl linoleate	220.68	216.43 [41]			252.99 [21]
		217.94 [22]			254.09 [25]
		220.68 [21]			258.15[b]

[a] Uncertainties for temperature and pressure are ±0.30 K and ±0.1 kPa, respectively.
[b] Values cited in the work published by Knothe and Dunn, 2009 [41].

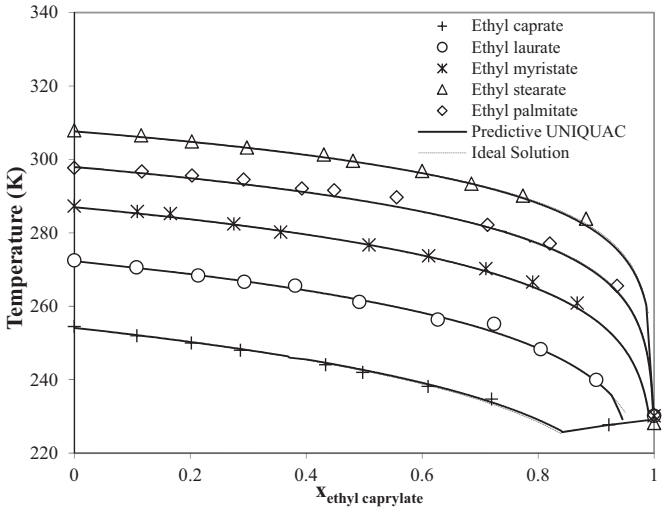

Fig. 1. *Liquidus* lines of binary mixtures formed by ethyl caprate, ethyl laurate, ethyl myristate, ethyl palmitate and ethyl stearate with ethyl caprylate. Symbols represent experimental melting points and lines represent calculated melting points.

the occurrence of a solid solution is observed just for a difference equal 4 in the binary mixtures formed by FAEE + ethyl caprate. One explanation is the ethyl caprylate molecule size that favours its interaction with the other FAEE of the mixture when compared with ethyl caprate molecule.

4.3. Phase diagrams with unsaturated FAEEs

The phase diagrams of ethyl laurate + ethyl oleate and ethyl myristate + ethyl oleate was published by Robustillo et al. [25,26] The results presented here for the same systems are in good agreement with the Robustillo and co-workers [25,26] presenting a relative deviation lower than 0.3 in average. The *liquidus* line of ethyl palmitate + ethyl oleate and ethyl stearate + ethyl oleate were previous published by us [21,22] and are presented again just for completeness, as mentioned before.

The phase diagrams of ethyl caprate, ethyl laurate and ethyl myristate with ethyl oleate present a well defined eutectic point at compositions of $x_{caprate} \cong 0.50$, $x_{laurate} \cong 0.80$, and $x_{myristate} \cong 0.95$, respectively, as can be seen in Fig. 5. In this set of data the system ethyl caprate + ethyl oleate exhibits a solid-solid transition for some compositions of the mixture that are reported in Table 5. The others systems of this set of data exhibit a temperature transition slightly above the eutectic one that may be related to the polymorphic transitions commonly found in fatty system [39,40].

The binary mixture equilibrium data of ethyl caprate, ethyl laurate and ethyl myristate with ethyl linoleate are presented in Table 6. Fig. 6 clearly shows a eutectic point formed by ethyl caprate + ethyl linoleate mixture in a composition of $x_{linoleate} \cong 0.90$ and the model result suggest the occurrence of a eutectic point in the system formed by ethyl laurate + ethyl linoleate at $x_{linoleate} \cong 0.98$.

A solid solution region was observed just for the system ethyl caprate with ethyl oleate in a region rich in the last one. It is possible that carbon chain of other saturated esters is so large to interact with the unsaturated ones and should be considered here the molecule package due to the unsaturation. In this way, all that can be observed in this set of phase diagrams is the eutectic point and a total immiscibility between both compounds in the solid phase, except for the system ethyl caprate + ethyl oleate.

The *liquidus* line of the phase diagrams presented in this study confirms that melting/cloud points are controlled by the heavier saturated FAEE while the unsaturated and light saturated FAEE, which present lower melting points, cause a very small decrease in the mixture melting temperature that can be related to cloud point.

Table 3
Melting and transition temperatures of binary mixtures formed by ethyl caprate (2), ethyl laurate (3) and ethyl myristate (4) with ethyl caprylate (1).[a]

Ethyl caprate (2) + ethyl caprylate (1)					Ethyl laurate (3) + ethyl caprylate (1)					Ethyl myristate(4) + ethyl caprylate (1)					
$x_{(caprylate)}$	$T_{eutectic}$	$T_{trans\ pure}$	$T_{melting}$	Solid phase	$x_{(caprylate)}$	$T_{eutectic}$	$T_{trans\ pure}$	$T_{melting}$	Solid phase	$x_{(caprylate)}$	T_{trans}	T_{trans}	$T_{trans\ pure}$	$T_{melting}$	Solid phase
0.0000			254.51	2	0.0000			272.59	3	0.0000			286.40	287.37	4
0.1079	225.32		251.98	2	0.1070	227.43		270.62	3	0.1088	228.37	229.36		285.93	4
0.2018	225.67		250.01	2	0.2137	227.84		268.40	3	0.1657	228.63	229.62		285.05	4
0.2865	225.87		248.01	2	0.2929	227.96		266.69	3	0.2750	228.78	229.74		281.95	4
0.4333	226.00		244.10	2	0.3809	228.22		265.61	3	0.3559	228.86	229.84		280.19	4
0.4975	225.99		242.00	2	0.4916	228.23		261.21	3	0.5083	228.89	229.71		277.33	4
0.6102	226.03		238.14	2	0.6270	228.30		256.39	3	0.6113	229.01	230.00		273.75	4
0.7195	225.75		234.72	2	0.7237	228.29		255.23	3	0.7099	229.11	230.04		270.24	4
0.9219	225.68		227.71	1	0.8041	228.19		248.33	3	0.7905	229.00	230.08		266.59	4
1.0000		229.18	230.35	1	0.9000	227.96		239.93	3	0.8675	229.15	230.10		259.53	4
					1.0000		229.18	230.35	1	1.0000			229.18	230.35	1

[a] Uncertainties for molar fraction, temperature and pressure are ±0.0005, ±0.30 K and ±0.1 kPa, respectively.

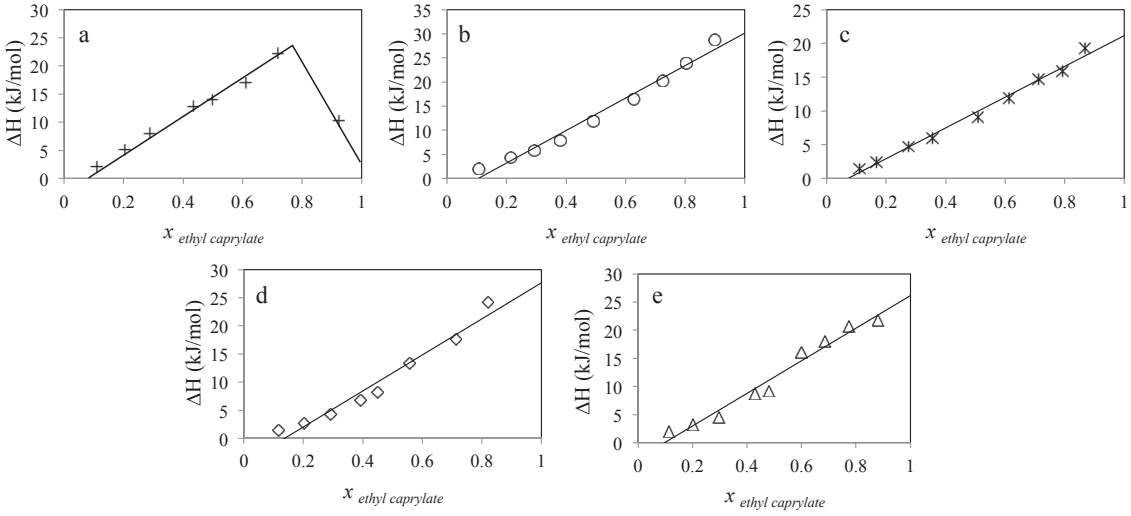

Fig. 2. Tammann plot of binary mixtures formed by: a) ethyl caprate + ethyl caprylate; b) ethyl laurate + ethyl caprylate; c) ethyl myristate + ethyl caprylate; d) ethyl palmitate + ethyl caprylate; e) ethyl stearate + ethyl caprylate. (solid lines are guide to the eyes).

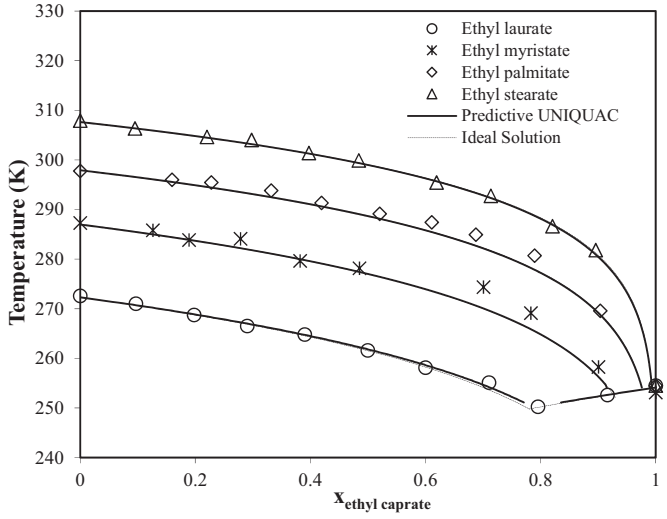

Fig. 3. *Liquidus* lines of binary mixtures formed by ethyl laurate, ethyl myristate, ethyl palmitate and ethyl stearate with ethyl caprate. Symbols represent experimental melting points and lines represent calculated melting points.

As an example, it is necessary to add to the mixture around 20% of the unsaturated and light saturated FAEE to notice a decrease of 5° in melting temperature of the mixture. This amount suggests that solvent addition is not the most feasible way to improve the cloud point property of biodiesel.

4.4. Thermodynamic modeling

The solid lines showed in the Figures are the Predictive UNIQUAC model results of the melting points and give an excellent description of the experimental results with an average deviation lower than 0.5 K. It is newsworthy note that even in very small temperatures, which are the case of systems formed by ethyl oleate or ethyl linoleate, the model predictions are pretty accurate. Additionally the results of this study are in accordance with literature data published for fatty acid methyl ester mixtures [33] and once again confirms the model capacity to predict the biodiesel behavior at lower temperatures.

Besides the predictive UNIQUAQ model it was also considered the ideal approach to both pure solid and liquid phases. This approach is also predictive requiring just the melting temperature and enthalpy of pure compounds as information to be provided to the model and the T-*x* relation is given by Equation (6). Despite of the expectations the ideal model results, represented in the phase diagrams of Figs. 1, 3 and 5 by dashed lines, were as good as those

Table 4
Melting and transition temperatures of binary mixtures formed by ethyl laurate (3) and ethyl myristate (4) with ethyl caprate (2).[a]

Ethyl laurate (3) + ethyl caprate (2)					Ethyl myristate (4) + ethyl caprate (2)					
$x_{(caprate)}$	$T_{eutectic}$	T_{trans}	$T_{melting}$	Solid phase	$x_{(caprate)}$	T_{trans}	$T_{eutectic}$	$T_{trans\ pure}$	$T_{melting}$	Solid phase
0.0000			272.59	3	0.0000			286.40	287.37	4
0.0967	249.23		271.01	3	0.1264		252.12		285.81	4
0.1979	249.49		268.74	3	0.1891		25208		283.84	4
0.2901	249.56	247.38	266.51	3	0.2786		252.23		284.08	4
0.3901	249.57	247.16	264.79	3	0.3822	251.02	252.32		279.61	4
0.4996	249.77	247.02	261.58	3	0.4854	250.90	252.33		278.15	4
0.6000	249.79	246.72	258.13	3	0.5996	250.98	252.23		274.02	4
0.7105	249.96	246.51	255.09	3	0.7830	251.16	252.12		267.49	4
0.7955		246.79	250.25	3, 2	0.9006	250.48			252.15	4
0.9160	249.98		252.61	2	1.0000				254.51	2
1.0000			254.51	2						

[a] Uncertainties for molar fraction, temperature and pressure are ±0.0005, ±0.30 K and ±0.1 kPa, respectively.

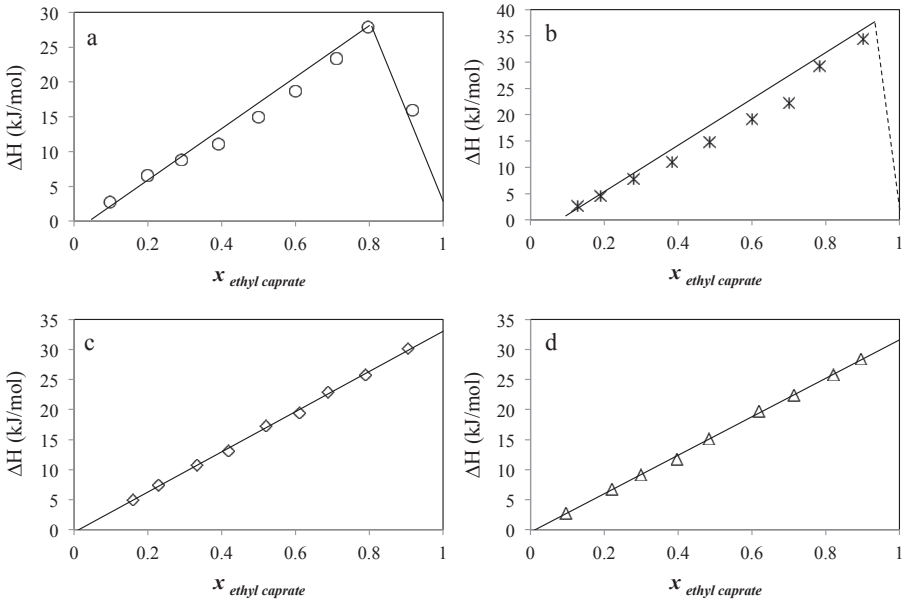

Fig. 4. Tammann plot of binary mixtures formed by: a) ethyl laurate + ethyl caprate; b) ethyl myristate + ethyl caprate; c) ethyl palmitate + ethyl caprate; d) ethyl stearate + ethyl caprate (solid and dashed lines are guide to the eyes).

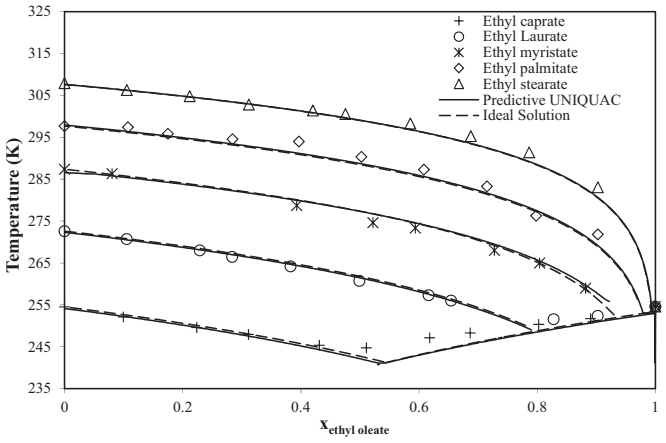

Fig. 5. *Liquidus* lines of binary mixtures formed by ethyl caprate, ethyl laurate, ethyl myristate, ethyl palmitate and ethyl stearate with ethyl oleate. Symbols represent experimental melting points and lines represent calculated melting points.

Table 5
Melting and transition temperatures of binary mixture formed by ethyl caprate (2) with ethyl oleate (5).[a]

Ethyl caprate (2) + ethyl oleate (5)				
$x_{(caprate)}$	T_{trans}	$T_{eutectic}$	$T_{melting}$	Solid phase
0.0000			254.61	5
0.1097	237.59	242.65	251.69	5
0.1974	239.05	243.26	250.33	5
0.3134		243.51	248.30	5
0.3821		243.69	247.13	5
0.4891		243.89	244.72	5
0.5688	238.69	243.92	245.36	2
0.6885	238.42	244.07	247.92	2
0.7762	238.27	243.92	249.57	2
0.9007		243.59	252.09	2
1.0000			254.51	2

[a] Uncertainties for molar fraction, temperature and pressure are ±0.0005, ±0.30 K and ±0.1 kPa, respectively.

obtained using the Predictive UNIQUAC model. Nevertheless the ideal approach can hardly be applied to a Bx blend due to its composition singularity, or in other words, it will not allow the

Table 6
Melting and transition temperatures of binary mixtures formed by ethyl caprate (2), ethyl laurate (3) and ethyl myristate (4) with ethyl linoleate (6).[a]

Ethyl caprate (2) + ethyl linoleate (6)					Ethyl laurate (2) + ethyl linoleate (6)					Ethyl myristate (4) + ethyl linoleate (6)					
$x_{(linoleate)}$	$T_{eutectic}$	T_{trans}	$T_{melting}$	Solid phase	$x_{(linoleate)}$	$T_{eutectic}$	T_{trans}	$T_{melting}$	Solid phase	$x_{(linoleate)}$	T_{trans}	T_{trans}	T_{trans}	$T_{trans\ pure}$	$T_{melting}$	Solid phase
0.0000			254.51	2	0.0000			272.59	3	0.0000				286.40	287.37	4
0.0909	216.48	213.71	252.34	2	0.1080	214.70	217.57	270.29	3	0.0925	214.79	217.81			286.66	4
0.1694	216.81	213.55	250.71	2	0.2184	214.54	217.59	268.16	3	0.2078	214.89	218.00	219.95		284.06	4
0.2853	216.78	213.56	247.74	2	0.4176	215.00	217.96	262.79	3	0.3342	214.93	218.09	219.87		280.96	4
0.4333	217.06	213.96	243.69	2	0.5107	214.08	217.19	259.43	3	0.4098	215.15	218.27	220.06		278.62	4
0.6245	217.06	214.00	237.06	2	0.5800	214.78	217.86	257.36	3	0.4788	215.15	218.25	220.08		277.35	4
0.7028	217.03	213.78	232.67	2	0.7979	214.87	218.01	247.81	3	0.5826	215.10	218.3.0	220.02		273.50	4
0.7992	217.12	213.54	227.72	2	0.8966	214.71	218.05	238.78	3	0.7051	215.35	218.34	220.18		269.42	4
1.0000			220.68	6	1.0000			220.68	6	0.8202	215.39	218.51	220.17		261.85	4
										0.9026	215.31	218.45	220.14		255.13	4
										1.0000					220.68	6

[a] Uncertainties for molar fraction, temperature and pressure are ±0.0005, ±0.30 K and ±0.1 kPa, respectively.

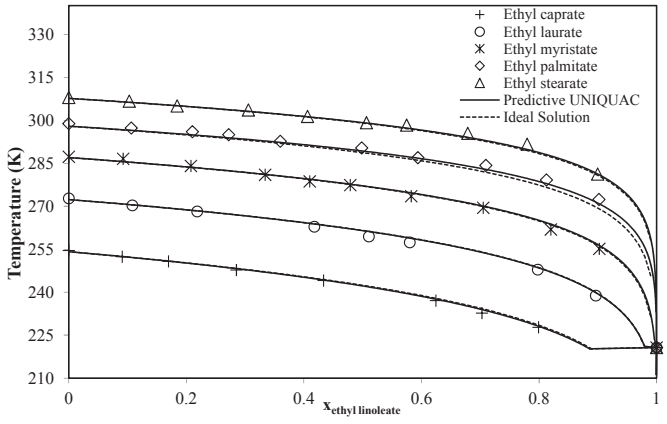

Fig. 6. *Liquidus* lines of binary mixtures formed by ethyl caprate, ethyl laurate, ethyl myristate, ethyl palmitate and ethyl stearate with ethyl linoleate. Symbols represent experimental melting points and lines represent calculated melting points.

prediction of cloud points of biodiesel using just its composition. This subject will be considered in a future work.

5. Conclusion

Nine solid-liquid phase diagrams of FAEE binary mixtures were studied by DSC and discussed in this work that complements solid-liquid equilibrium of FAEE studies. Moreover this work confirms that higher melting points saturated fatty esters are responsible by the undesired behavior of such a substances in low temperatures. It was confirmed that just the systems formed by ethyl myristate with ethyl palmitate and ethyl stearate are more complex due to the existence of the eutectic and peritectic points. Besides the experimental data determination it was successfully utilized the predictive UNIQUAC and ideal solution models to predict the melting temperatures of FAEE binary mixtures.

Acknowledgments

The authors thank to CNPq (479533/2013-0, 308616/2014-6 and 304495/2010-7), FAPESP (2012/05027-1), and FAEPEX/UNICAMP for funding the research. This work was developed in the scope of the project CICECO-Aveiro Institute of Materials (Ref. FCT UID/CTM/50011/2013), financed by national funds through the FCT/MEC and when applicable co-financed by FEDER under the PT2020 Partnership Agreement.

Appendix A. Supplementary data

Supplementary data related to this article can be found at http://dx.doi.org/10.1016/j.fluid.2016.06.039.

References

[1] M. Lapuerta, J. Rodríguez-Fernández, J.R. Agudelo, Diesel particulate emissions from used cooking oil biodiesel, Bioresour. Technol. 99 (2008) 731–740.
[2] A.K. Agarwal, Biofuels (alcohols and biodiesel) applications as fuels for internal combustion engines, Prog. Energy Combust. Sci. 33 (June 2007) (2007) 233–271.
[3] J.K. Kim, E. Yim, C. Jeon, C.S. Jung, B. Han, Cold performance of various biodiesel fuel blends at low temperature, Int. J. Automot. Technol. 13 (2012) 293–300.
[4] R.O. Dunn, Effects of minor constituents on cold flow properties and performance of biodiesel, Prog. Energy Combust. Sci. 35 (2009) 481–489.
[5] M. Benziane, K. Khimeche, I. Mokbel, A. Dahmani, J. Jose, Isothermal vapor-liquid equilibria of n-tetradecane plus ethyl hexanoate, ethyl decanoate, and ethyl tetradecanoate, J. Chem. Eng. Data 58 (2013) 492–498.
[6] M. Benziane, K. Khimeche, I. Mokbel, T. Sawaya, A. Dahmani, J. Jose, Experimental vapor pressures of five saturated fatty acid ethyl ester (FAEE) components of biodiesel, J. Chem. Eng. Data 56 (2011) 4736–4740.
[7] N.D.D. Carareto, C.Y.C.S. Kimura, E.C. Oliveira, M.C. Costa, A.J.A. Meirelles, Flash points of mixtures containing ethyl esters or ethylic biodiesel and ethanol, Fuel 96 (2012) 319–326.
[8] R.C. Basso, A.J.D. Meirelles, E.A.C. Batista, Densities and viscosities of fatty acid ethyl esters and biodiesels produced by ethanolysis from palm, canola, and soybean oils: experimental data and calculation methodologies, Ind. Eng. Chem. Res. 52 (2013) 2985–2994.
[9] R. Ceriani, C.B. Goncalves, J. Rabelo, M. Caruso, A.C.C. Cunha, F.W. Cavaleri, E.A.C. Batista, A.J.A. Meirelles, Group contribution model for predicting viscosity of fatty compounds, J. Chem. Eng. Data 52 (2007) 965–972.
[10] R. Ceriani, F.R. Paiva, C.B. Goncalves, E.A.C. Batista, A.J.A. Meirelles, Densities and Viscosities of vegetable oils of nutritional value, J. Chem. Eng. Data 53 (2008) 1846–1853.
[11] C.B. Goncalves, R. Ceriani, J. Rabelo, M.C. Maffia, A.J.A. Meirelles, Viscosities of fatty mixtures: experimental data and prediction, J. Chem. Eng. Data 52 (2007) 2000–2006.
[12] L.Y.A. Silva, R.M.M. Falleiro, A.J.A. Meirelles, M.A. Krahenbuhl, Determination of the vapor pressure of ethyl esters by Differential Scanning Calorimetry, J. Chem. Thermodyn. 43 (2011) 943–947.
[13] L.Y.A. Silva, R.M.M. Falleiro, A.J.A. Meirelles, M.A. Krahenbuhl, Vapor-liquid equilibrium of fatty acid ethyl esters determined using DSC, Thermochim. Acta 512 (2011) 178–182.
[14] R. Ceriani, A.J.A. Meirelles, Predicting vapor-liquid equilibria of fatty systems, Fluid Phase Equilib. 215 (2004) 227–236.
[15] R.M. Joshi, M.J. Pegg, Flow properties of biodiesel fuel blends at low temperatures, Fuel 86 (2007) 143–151.
[16] M.I. Arbab, H.H. Masjuki, M. Varman, M.A. Kalam, H. Sajjad, S. Imtenan, Performance and emission characteristics of a diesel engine fueled by an optimum biodiesel-biodiesel blend, Rsc Adv. 4 (2014) 37122–37129.
[17] H. Imahara, E. Minami, S. Saka, Thermodynamic study on cloud point of biodiesel with its fatty acid composition, Fuel 85 (2006) 1666–1670.
[18] M. Tadie, I. Bahadur, P. Reddy, P.T. Ngema, P. Naidoo, N. Deenadayalu, D. Ramjugernath, Solid-liquid equilibria measurements for binary systems comprising (butyric acid plus propionic or pentanoic acid) and (heptanoic acid plus propionic or butyric or pentanoic or hexanoic acid), J. Chem. Thermodyn. 57 (2013) 485–492.
[19] M.D. Torres, G. Jiménez-Osés, J.A. Mayoral, E. Pires, Fatty acid derivatives and their use as CFPP additives in biodiesel, Bioresour. Technol. 102 (2011)

2590–2594.
[20] T.Q. Chastek, Improving cold flow properties of canola-based biodiesel, Biomass Bioenerg. 35 (2011) 600–607.
[21] L. Boros, M.L.S. Batista, R.V. Vaz, B.R. Figueiredo, V.F.S. Fernandes, M.C. Costa, M.A. Krähenbühl, A.J.A. Meirelles, J.A.P. Coutinho, Crystallization behavior of mixtures of fatty acid ethyl esters with ethyl stearate, Energy & Fuels 23 (2009) 4625–4629.
[22] M.C. Costa, L.A.D. Boros, M.L.S. Batista, J.A.P. Coutinho, M.A. Krahenbuhl, A.J.A. Meirelles, Phase diagrams of mixtures of ethyl palmitate with fatty acid ethyl esters, Fuel 91 (2012) 177–181.
[23] M.D. Robustillo, D.F. Barbosa, A.J.A. Meirelles, P.D.A. Filho, Solid-liquid equilibrium in ternary mixtures of ethyl laurate, ethyl palmitate and ethyl myristate, Fluid Phase Equilib. 361 (2014) 188–199.
[24] M.D. Robustillo, D.F. Barbosa, A.J.D. Meirelles, P.D. Pessoa, Solid-liquid equilibrium in ternary mixtures of ethyl laurate, ethyl palmitate and ethyl stearate, Fluid Phase Equilib. 358 (2013) 272–281.
[25] M.D. Robustillo, D.F. Barbosa, A.J.D. Meirelles, P.D. Pessoa, Solid-liquid equilibrium in ternary mixtures of ethyl oleate, ethyl laurate and ethyl palmitate, Fluid Phase Equilib. 339 (2013) 58–66.
[26] M.D. Robustillo, D.F. Barbosa, A.J.D. Meirelles, P.D. Pessoa, Solid-liquid equilibrium of binary and ternary mixtures containing ethyl oleate, ethyl myristate and ethyl stearate, Fluid Phase Equilib. 370 (2014) 85–94.
[27] M.C. Costa, M.P. Rolemberg, L.A.D. Boros, M.A. Krähenbühl, M.G. Oliveira, A.J.A. Meirelles, Solid-liquid equilibrium of binary fatty acids mixtures, J. Chem. Eng. Data 52 (2007) 30–36.
[28] J.A.P. Coutinho, J.L. Daridon, Low-pressure modeling of wax formation in crude oils, Energy & Fuels 15 (2001) 1454–1460.
[29] J.A.P. Coutinho, C. Dauphin, J.L. Daridon, Measurements and modelling of wax formation in diesel fuels, Fuel 79 (2000) 607–616.
[30] M.C. Costa, M.A. Krähenbühl, A.J.A. Meirelles, J.L. Daridon, J. Pauly, J.A.P. Coutinho, High pressure solid-liquid equilibria of fatty acids, Fluid Phase Equilib. 253 (2007) 118–123.
[31] M.C. Costa, L.A.D. Boros, J.A.P. Coutinho, M.A. Krahenbuhl, A.J.A. Meirelles, Low-temperature behavior of biodiesel: solid-liquid phase diagrams of binary mixtures composed of fatty acid methyl esters, Energy & Fuels 25 (2011) 3244–3250.
[32] J.A.P. Coutinho, M. Goncalves, M.J. Pratas, M.L.S. Batista, V.F.S. Fernandes, J. Pauly, J.L. Daridon, Measurement and modeling of biodiesel cold-flow properties, Energy & Fuels 24 (2010) 2667–2674.
[33] J.C.A. Lopes, L. Boros, M.A. Krahenbuhl, A.J.A. Meirelles, J.L. Daridon, J. Pauly, I.M. Marrucho, J.A.P. Coutinho, Prediction of cloud points of biodiesel, Energy & Fuels 22 (2008) 747–752.
[34] B.L. Larsen, P. Rasmussen, A. Fredenslund, A modified unifac group-contribution model for prediction of phase-equilibria and heats of mixing, Ind. Eng. Chem. Res. 26 (1987) 2274–2286.
[35] J.A.P. Coutinho, F. Mirante, J. Pauly, A new predictive UNIQUAC for modeling of wax formation in hydrocarbon fluids, Fluid Phase Equilib. 247 (2006) 8–17.
[36] J.A.P. Coutinho, Predictive UNIQUAC: a new model for the description of multiphase solid-liquid equilibria in complex hydrocarbon mixtures, Ind. Eng. Chem. Res. 37 (1998) 4870–4875.
[37] G.G. Chernik, Phase-Equilibria in phospholipid water-systems, Adv. Colloid Interface Sci. 61 (1995) 65–129.
[38] M.C. Costa, M. Sardo, M.P. Rolemberg, J.A.P. Coutinho, A.J.A. Meirelles, P. Ribeiro-Claro, M.A. Krähenbühl, The solid-liquid phase diagrams of binary mixtures of consecutive, even saturated fatty acids, Chem. Phys. Lipids 160 (2009) 85–97.
[39] E. Moreno, R. Cordobilla, T. Calvet, M.A. Cuevas-Diarte, G. Gbabode, P. Negrier, D. Mondieig, H.A.J. Oonk, Polymorphism of even saturated carboxylic acids from n-decanoic to n-eicosanoic acid, New J. Chem. 31 (2007) 947–957.
[40] G.J. Maximo, M.C. Costa, J.A.P. Coutinho, A.J.A. Meirelles, Trends and demands in the solid-liquid equilibrium of lipidic mixtures, Rsc Adv. 4 (2014) 31840–31850.
[41] G. Knothe, R.O. Dunn, A comprehensive evaluation of the melting points of fatty acids and esters determined by differential scanning calorimetry, J. Am. Oil Chemists' Soc. 86 (2009) 843–856.
[42] E.W. Lemmon, M.O. McLinden, D.G. Friend, Thermophysical properties of fluid systems, in: P.J. Linstrom, W.G. Mallard (Eds.) NIST Chemistry WebBook, NIST Standard Reference Database Number 69, National Institute of Standards and Technology, Gaithersburg.